

# Identification and Regulation of Whole-Cell Chloride Currents in Airway Epithelium

JOHN D. McCANN, MING LI, and MICHAEL J. WELSH

From the Howard Hughes Medical Institute, Department of Internal Medicine, University of Iowa College of Medicine, Iowa City, Iowa 52242

**ABSTRACT** We used the whole-cell patch-clamp technique to study membrane currents in human airway epithelial cells. The conductive properties, as described by the instantaneous current-voltage relationship, rectified in the outward direction when bathed in symmetrical CsCl solutions. In the presence of Cl concentration gradients, currents reversed near  $E_{Cl}$  and were not altered significantly by cations. Agents that inhibit the apical membrane Cl conductance inhibited Cl currents. These conductive properties are similar to the conductive properties of the apical membrane Cl channel studied with the single-channel patch-clamp technique. The results suggest that the outwardly rectifying Cl channel is the predominant Cl-conductive pathway in the cell membrane. The steady-state and non-steady-state kinetics indicate that current flows through ion channels that are open at hyperpolarizing voltages and close with depolarization. These Cl currents were regulated by the cAMP-dependent protein kinase: when the catalytic subunit of cAMP-dependent protein kinase was included in the pipette solution, Cl channel current more than doubled. We also found that reducing extracellular osmolarity by 30% increased Cl current, suggesting that cell-swelling stimulated Cl current. Studies of transepithelial Cl transport in cell monolayers suggest that a reduction in solution osmolarity activates the apical Cl channel: reducing extracellular osmolarity stimulated a short-circuit current that was inhibited by Cl-free solution, by mucosal addition of a Cl channel antagonist, and by submucosal addition of a loop diuretic. These results suggest that apical membrane Cl channels may be regulated by cell volume and by the cAMP-dependent protein kinase.

## INTRODUCTION

Airway epithelia secrete Cl from the submucosal to the mucosal surface. Cl enters the cell at the basolateral membrane via a neutral cotransport process and exits the cell through an apical membrane Cl channel (Welsh, 1987*b*). Neuro-humoral agents control the rate of transepithelial Cl secretion, at least in part, by regulating apical membrane Cl channels. cAMP is thought to regulate Cl channels, because many agents that stimulate Cl secretion and open apical Cl channels increase cellular con-

Address reprint requests to Dr. Michael J. Welsh, Department of Internal Medicine, University of Iowa College of Medicine, Iowa City, IA 52242.

centrations of cAMP. In addition, secretion is stimulated by membrane-permeable analogues of cAMP, and agents that increase cellular cAMP levels by activating adenylate cyclase or inhibiting phosphodiesterase.

The purpose of this study was twofold. The first goal was to adapt the whole-cell patch-clamp technique (Marty and Neher, 1983) to the study of Cl channel currents in human airway epithelium. This technique has proven valuable in understanding the properties and regulation of ion channels in many excitable cells. The second goal was to use this technique to investigate regulation of the apical Cl channel. Because cAMP is important in regulating Cl secretion, and because many of the cellular effects of cAMP are mediated by cAMP-dependent protein kinase (Nestler and Greengard, 1984), we tested the hypothesis that the Cl channel is regulated by cAMP-dependent protein kinase. During the course of these studies we found that decreasing extracellular osmolarity can also activate Cl currents. Given this new observation we tested the hypothesis that the apical membrane Cl conductance of the intact epithelium can also be regulated by changes in cell volume.

#### METHODS

The methods for obtaining and enzymatically dispersing human airway epithelial cells have been described elsewhere (Coleman et al., 1984; Welsh, 1985*b*). Cells were either plated immediately after isolation or were stored in liquid nitrogen for 5–90 d before plating. After isolation, we placed cells in cryogenic vials at a concentration of  $1.5 \times 10^7$  cells/ml in a solution consisting of 90% culture medium (described below) and 10% dimethylsulfoxide (DMSO). The vials were cooled from room temperature to  $-70^\circ\text{C}$  at a rate of  $\sim 1^\circ\text{C}/\text{min}$ , then transferred to liquid nitrogen for storage. To thaw the cells, we placed the vials in a  $37^\circ\text{C}$  water bath for 4–5 min. The thawed cell medium with 10% DMSO was diluted to 16–19 ml with regular medium and centrifuged at 100 *g* for 10 min. Afterwards, the cells were washed with culture media and centrifuged a second time, then the cell pellet was suspended in 3–4 ml of medium. After thawing, cell viability was 70–75%. Cells stored in liquid nitrogen before plating had morphology, transepithelial electrical properties, hormonal responsiveness, and single-channel properties that were the same as those observed with cells that had not been frozen (Welsh, 1985*b*).

Cells were plated on collagen-coated 35-mm tissue culture dishes (Costar, Cambridge, MA) or collagen-coated plastic coverslips at a seeding density between  $10^4$  and  $10^5$  cells/cm<sup>2</sup>. The culture medium consisted of a 1:1 mixture of Dulbecco's modified Eagles medium that contained 1 g/liter glucose and Ham's F-12 medium. The medium was supplemented with 5% fetal calf serum, 100 U/ml penicillin, 100  $\mu\text{g}/\text{ml}$  streptomycin, and 5  $\mu\text{g}/\text{ml}$  insulin. Cells were incubated at  $37^\circ\text{C}$  and 5% CO<sub>2</sub> for 2–3 d before the studies.

Methods used for single-channel studies were identical to those described elsewhere (Hamill et al., 1981; Welsh, 1986*a, b*). The methods for whole-cell studies were similar to those described by Marty and Neher (1983). We pulled whole-cell pipettes in a two stage process from 100  $\mu\text{l}$  disposable micropipettes (Rochester Scientific Co. Inc., Rochester, NY) on a pipette puller (model 750; David Kopf Instruments, Tulumga, CA). After fire-polishing, pipettes had a resistance of  $3.17 \pm 0.08 \text{ M}\Omega$  ( $n = 165$ ). Tissue culture dishes were mounted directly on the stage of an inverted microscope (Leitz Diavert, FRG), which sat on a vibration isolation table (model XJ-A; Newport Corp., Fountain Valley, CA). A PDP 11/73 laboratory computer and interface (Indec Systems Inc., Sunnyvale, CA) used software written in this laboratory in BASIC23 for voltage stimulation, current sampling, and data analysis. We sampled currents at 5 kHz and low-pass filtered them at 2.5 kHz with an eight-pole Bessel filter (Frequency Devices Inc., Haverhill, MA).

Only single, isolated cells were studied. Previous studies using the single-channel patch-clamp technique have demonstrated the presence of apical  $\text{Cl}^-$  channels in single, isolated human and canine airway epithelial cells (Frizzell et al., 1986; Welsh, 1986*a, b*; Welsh and Liedtke, 1986; Schoumacher et al., 1987; Li et al., 1988). Light suction to the pipette interior facilitated formation of seals with resistances of  $6.24 \pm 0.32 \text{ G}\Omega$  ( $n = 165$ ). After sealing, the patch was held at  $-60 \text{ mV}$  and 20-ms pulses to  $-75 \text{ mV}$  were applied while we cancelled the pipette capacitance using the analogue circuitry of the voltage clamp (model EPC7; List Medical Electronic, Darmstadt, FRG). Applying more forceful suction to the pipette interior, we ruptured the membrane beneath the pipette. The cell capacitance,  $26.3 \pm 0.7 \text{ pF}$  ( $n = 165$ ), was cancelled using the analogue circuitry within the voltage clamp. The series resistance,  $7.54 \pm 0.24 \text{ M}\Omega$  ( $n = 165$ ), could typically be maintained without application of negative pressure. In a few experiments continuous negative pressure was necessary to reduce series resistance. Estimates of series resistance were rechecked intermittently throughout the experiment. Voltages are referenced to the outside of the cell and outward currents represent anions flowing into the cell.

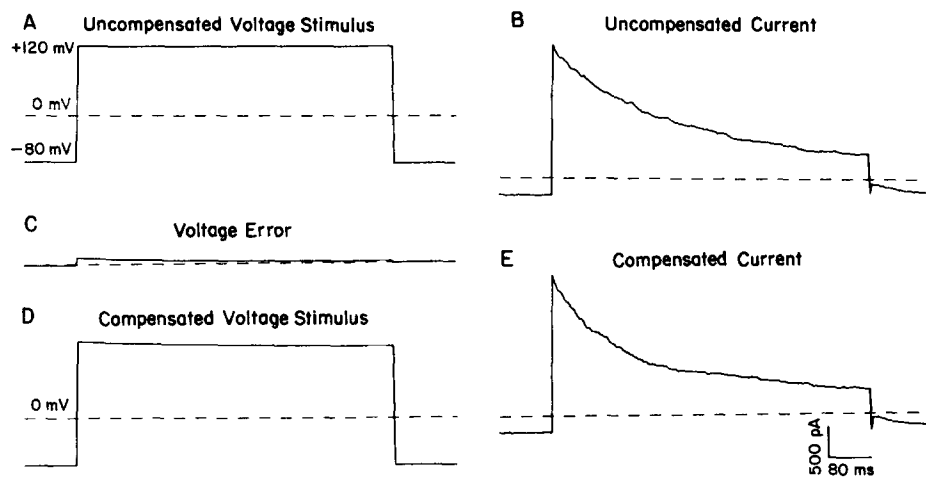


FIGURE 1. Method for compensating series resistance. Dashed line represents zero current in the current tracings. The series resistance is  $5.3 \text{ M}\Omega$ . See text for details.

Because we had large currents (sometimes  $>3 \text{ nA}$ ) and because it was technically difficult to decrease series resistance by using lower resistance pipettes, we compensated for the voltage drop across the series resistance digitally, using a two-step algorithm. Fig. 1 shows an example of the method using currents from a cell with qualitatively and quantitatively representative currents. Holding voltage was  $-80 \text{ mV}$  and target voltage was  $+120 \text{ mV}$ . During the first step, this algorithm gave the uncompensated square-wave command voltage stimulus, Fig. 1 A. The resulting current points are shown in Fig. 1 B; this tracing would not be saved because it is uncompensated. The current points were then multiplied by the series resistance to obtain an estimate of the voltage drop (error) across the series resistance, Fig. 1 C. In the second step, this estimate, Fig. 1 C, was summed with the command voltage, Fig. 1 A, to provide the compensated voltage stimulus, Fig. 1 D. Fig. 1 E shows the currents in response to the compensated voltage stimulus. Comparison of the currents in Fig. 1, B and E shows that this method gives the same result that would be expected from analogue series resistance compensation. Note that the compensation increases the peak current amplitude and, as one would expect (see below), this increase in voltage accentuates the decay of currents observed

with strong depolarizing voltages. A disadvantage of this digital method is that we had to discard the current points from step one, since the command voltage stimulus was uncompensated during that step. However, this protocol allowed us to compensate for the voltage drop across the series resistance without amplifier oscillation, which often limits analogue series resistance compensation.

Unless otherwise indicated the standard pipette solution contained in millimolar: 135 CsCl, 2 MgCl<sub>2</sub>, 1 MgATP, 5 EGTA/0.31 CaCl<sub>2</sub> (free [Ca] = 10<sup>-8</sup> M), 10 HEPES, titrated to pH 7.2 with ~20 CsOH. The standard extracellular NaCl solution contained in millimolar: 135 NaCl, 1.2 MgCl<sub>2</sub>, 1.2 CaCl<sub>2</sub>, 10 HEPES, titrated to pH 7.4 with ~5 KOH. The standard extracellular CsCl solution contained in millimolar: 135 CsCl, 1.2 MgCl<sub>2</sub>, 1.2 CaCl<sub>2</sub>, 10 HEPES, titrated to pH 7.4 with ~5 CsOH.

For studies examining the effect of 5-nitro-2-(3-phenylpropylamino)-benzoate (NPPB) and the effect of reduced extracellular osmolarity, canine tracheal epithelial cells were cultured as monolayers on permeable supports and mounted in modified Ussing chambers (Welsh, 1985*b*). The bathing solution contained in millimolar: 135 NaCl, 1.2 MgCl<sub>2</sub>, 1.2 CaCl<sub>2</sub>, 2.4 K<sub>2</sub>HPO<sub>4</sub>, 0.6 KH<sub>2</sub>PO<sub>4</sub>, 10 dextrose, and 10 HEPES (pH 7.4 with NaOH). The mucosal solution contained amiloride (10 μM), so that the short-circuit current reflected primarily Cl secretion. For studying the effect of NPPB, Cl secretion was stimulated with epinephrine (5 μM). For studies examining the effect of osmolarity, we diluted the 2 ml of mucosal and submucosal solution with 1 ml of a solution of identical composition except that it contained no NaCl.

Drugs used in this study include amiloride (a generous gift of Merck, Sharp and Dohme Research Laboratories, Westpoint, PA), alkaline phosphatase, type VII-L (Sigma Chemical Co., St. Louis, MO), DL-dithiothreitol (Sigma), guanosine 5'-triphosphate, type 1 Na salt (Sigma), adenosine 5'-triphosphate, Mg salt from equine muscle (Sigma), phosphocreatine, disodium salt (Sigma); protein kinase inhibitor from rabbit muscle (Sigma), diphenylamine-2-carboxylate (Fluka, Switzerland), and NPPB (a generous gift from Dr. R. Greger, Albert-Ludwig-Universität, Freiburg, FRG).

The catalytic subunit of cAMP-dependent protein kinase was prepared in the laboratory of Drs. Angus C. Nairn and Paul Greengard (Rockefeller University, New York, NY) from bovine heart as previously described (Kaczmarek et al., 1980). The protein kinase was stored refrigerated in an isotonic stock solution containing 150 mM KCL, 10 mM HEPES, pH 7.4 with KOH, which was diluted at least 1:100 before use.

## RESULTS

### *Conductive Properties of Cell Cl Currents*

The predominant conductances of airway epithelial cells are to Cl and K, with a small contribution from Na (Welsh, 1987*b*). To isolate whole-cell currents to Cl channels, we bathed and perfused cells with solutions that contained Cl as the major permeant ion. The predominant cation in the pipette was Cs and the predominant cation in the bathing solutions was either Cs or Na. (In previous single-channel studies we found that Cs did not alter the properties of the Cl channel, Welsh, 1986*b*.) In experiments in which Na was present we usually blocked Na currents with amiloride (10–100 μM).

To study the conductive properties of Cl currents, the holding voltage was maintained at –80 mV and membrane voltage was stepped to values between –90 and +120 mV. Voltages are referenced to the bathing solution and upward deflections represent outward current, which is carried by Cl flowing into the cell. Fig. 2 shows

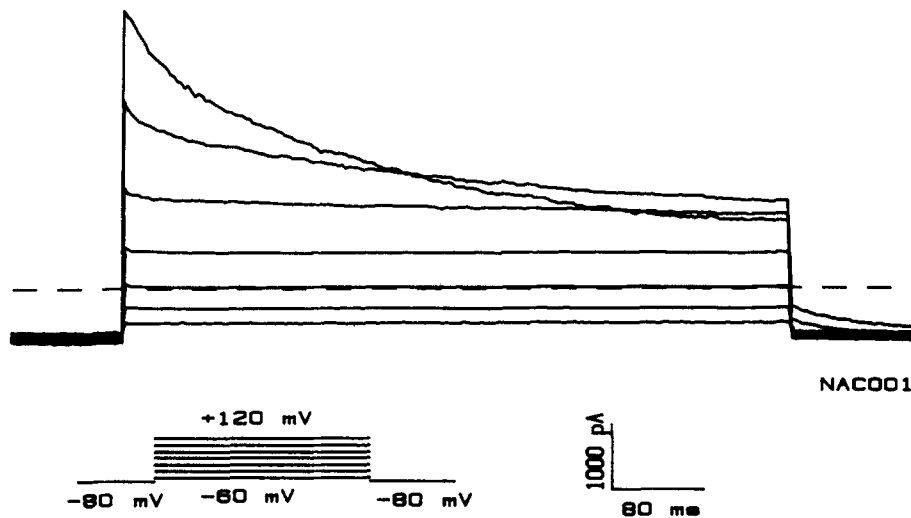


FIGURE 2. Representative example of whole-cell currents. Holding voltage of  $-80$  mV was maintained for 5 s and then voltage was stepped to values from  $-90$  to  $+120$  mV in increments of 30 mV, as shown in the inset. The dashed line indicates the zero-current level. The pipette (internal) solution was the standard CsCl pipette solution. The bath solution contained our standard extracellular NaCl solution plus  $100 \mu\text{M}$  amiloride.

that the increment in initial current for each 30-mV increment in voltage is greater with voltage steps to positive potentials than with voltage steps to negative potentials. In Fig. 3 the initial current is plotted vs. the target voltage. The instantaneous whole-cell current-voltage relationship rectifies in the outward direction. Apical membrane Cl channels from human airway epithelial cells show similar outward rectification in excised, inside-out patches bathed with symmetrical Cl solutions (Welsh, 1986*a, b*; Frizzell et al., 1986). Thus, whole-cell currents have conductive properties that would be predicted from single-channel studies.

To demonstrate that the current flows through Cl channels, we examined the effect of Cl concentration gradients; Fig. 4 shows the data. The slope of the regres-

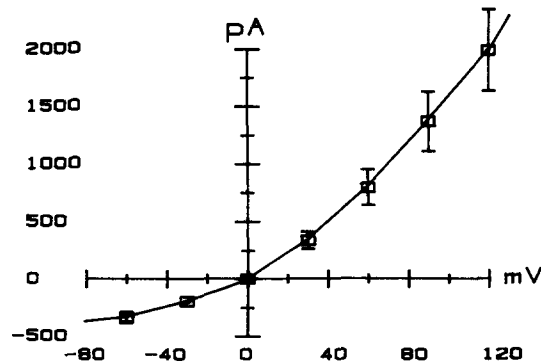


FIGURE 3. Current-voltage relationship of Cl channel currents. Current was measured 7 ms after voltage steps from a holding voltage of  $-80$  mV to the target voltage. Data are mean  $\pm$  SEM of 14 cells from four different preparations. The internal solution was our standard CsCl pipette solution except that MgATP was not included, and the external solution was our standard CsCl bath solution.

sion line is 49 mV with a slope of 58 mV expected from the Nernst equation. Total cell current is composed of both Cl channel current and "leak" current, i.e., that current which flows through other channels and around the pipette-membrane seal. It was not possible to subtract leak current from total current used to determine reversal potential. Because the leak currents reversed near 0 mV (see discussion below), the inclusion of some leak current has the effect of reducing the absolute value of the measured reversal potentials. Hence the slope of the line shown in Fig. 4 is less than the true slope for the Cl channel and the whole-cell currents are more Cl-selective than the data in Fig. 4 indicates. When cells were bathed in symmetrical 155 mM Cl with Na as the cation in the bath and Cs the cation in the pipette, the currents reversed at +2 mV indicating that even in the absence of amiloride very little current was carried by Na.

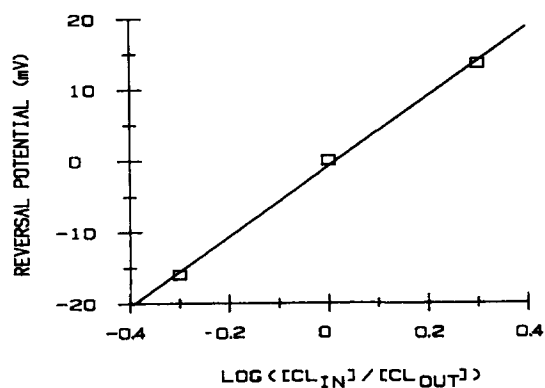


FIGURE 4. Effect of Cl concentration gradients on the reversal potential of whole-cell currents. Data from two sets of experiments are included. In the first set, the pipette contained a solution with 77.5 mM Cl (Cs the dominant cation) and the bath contained 155 mM Cl (Cs the dominant cation,  $n = 4$ ). In the second set of experiments the pipette contained 155 mM Cl (Cs the

dominant cation) and during seal formation and rupture of the membrane patch the bathing solution contained the standard extracellular NaCl solution. The bathing solution was switched to one containing 155 mM Cl (Cs the dominant cation) and then to 77.5 mM Cl (Cs the dominant cation and osmolarity maintained with mannitol,  $n = 3$ ). The slope of the regression line is 49 mV.

#### *Effect of Membrane Voltage on Cl Channel Currents*

We now return to Fig. 2 to consider the kinetic properties of the current. On stepping to voltages more positive than +30 mV, currents decayed during the 600-ms pulse. The rate of decay was variable from preparation to preparation, but in any given cell it was always more rapid at +120 mV than at +90 or +60 mV. At first inspection, it would appear that depolarizing voltage steps are causing channels to open and then subsequently close, or decay, with time. Such an interpretation suggests behavior similar to that of Na or Ca channels in excitable membranes. However, closer inspection shows that this is not the case for Cl channel currents: channels are open at the holding voltage of -80 mV and close with strong depolarization. Three lines of evidence support this conclusion.

First, whole-cell currents peak and immediately begin to decay after depolarizing voltage steps. If Cl channels were opened by depolarization, the peak current would not occur immediately after the voltage step.

Second, depolarization decreased cell conductance. Fig. 5 A shows the effect of stepping voltage from a holding potential of  $-80$  to  $+120$  mV for different durations. The longer the voltage is maintained at  $+120$  mV, the greater the current decay. More importantly, the absolute value of the tail current observed upon

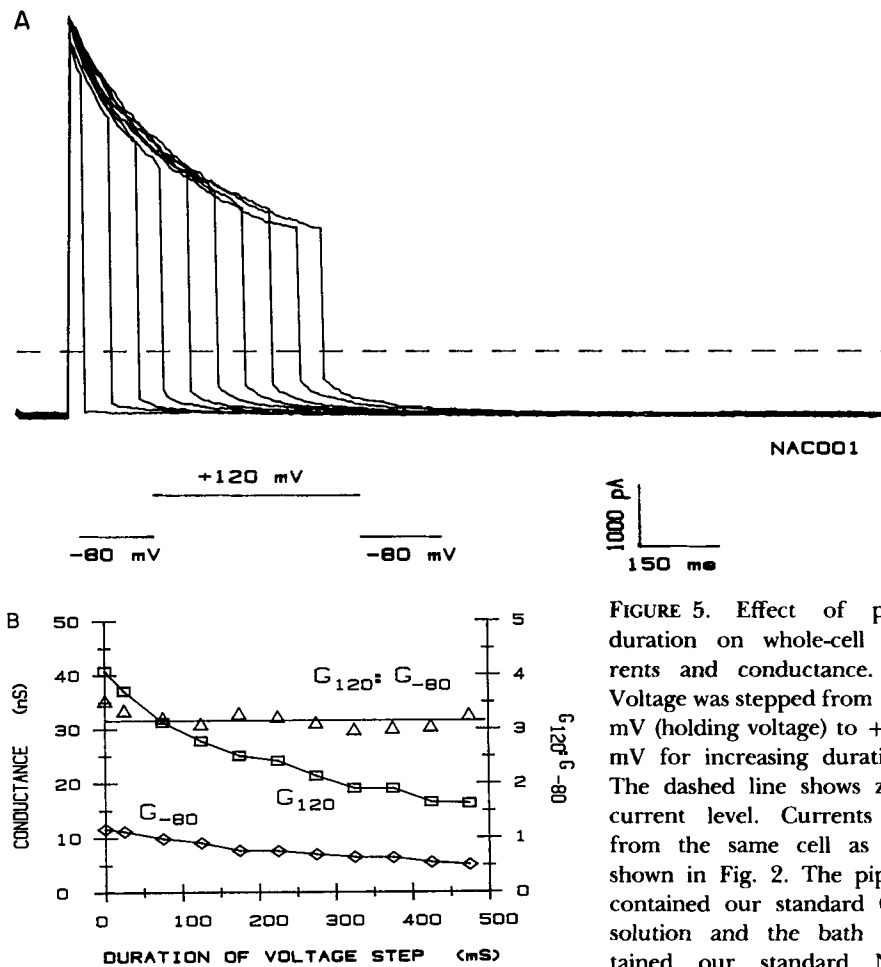


FIGURE 5. Effect of pulse duration on whole-cell currents and conductance. (A) Voltage was stepped from  $-80$  mV (holding voltage) to  $+120$  mV for increasing durations. The dashed line shows zero-current level. Currents are from the same cell as that shown in Fig. 2. The pipette contained our standard CsCl solution and the bath contained our standard NaCl

extracellular solution plus  $100 \mu\text{M}$  amiloride. The point at zero duration was obtained by measuring the steady-state conductance at  $-80$  mV and the conductance immediately after the pulse to  $+120$  mV. (B) Data are from A. Conductance at  $120$  mV ( $G_{120}$ ) is measured at the end of the voltage steps to  $120$  mV (squares). Conductance at  $-80$  mV ( $G_{-80}$ ) is measured immediately after returning the membrane voltage from  $+120$  to  $-80$  mV (diamonds). Triangles show the ratio of conductance at  $120$  mV to that at  $-80$  mV ( $G_{120}:G_{-80}$ ).

returning to  $-80$  mV decreases as the duration at  $+120$  mV increases. Similar observations were made in seven cells.

Data shown in Fig. 5 B quantifies the observations made in Fig. 5 A. In Fig. 5 B we plot chord conductance at  $+120$  mV ( $G_{120}$ ), measured at the end of pulses to  $+120$

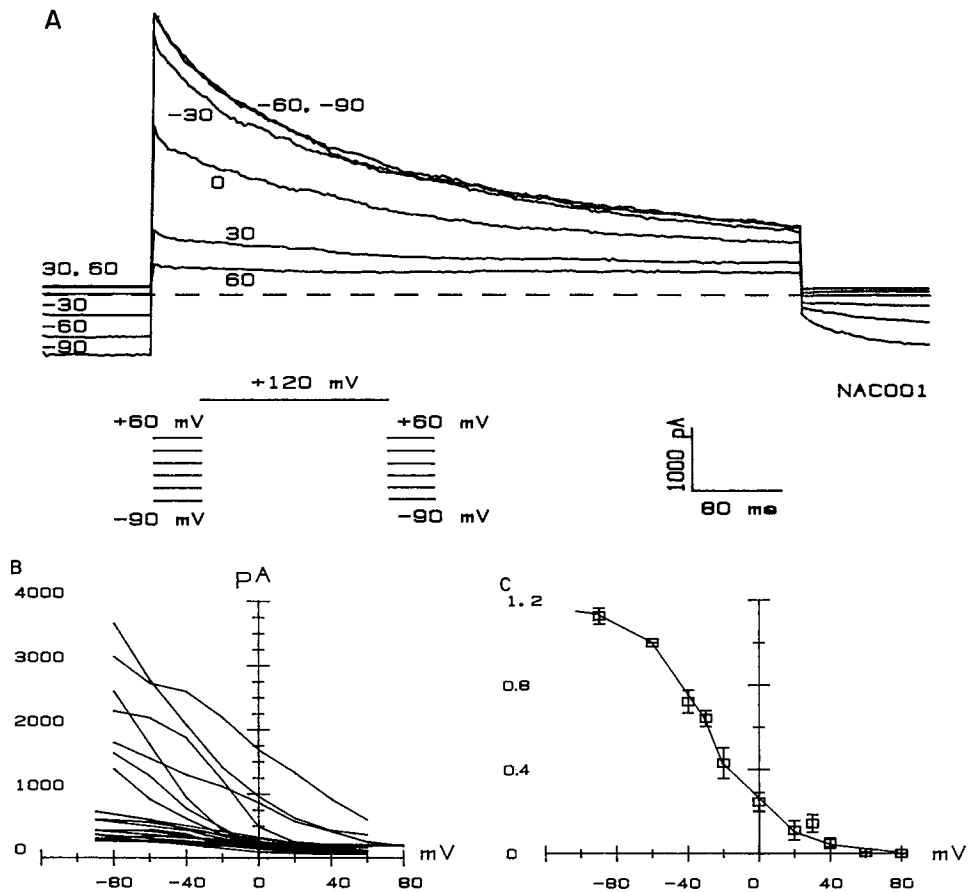


FIGURE 6. Effect of holding voltage on whole-cell currents. (A) Holding voltage was maintained for 5 s at values from  $-60$  to  $+60$  mV and then stepped to  $+120$  mV for 600 ms, as shown in the inset. Solutions were standard CsCl pipette solution and standard extracellular NaCl solution plus  $100 \mu\text{M}$  amiloride; the cell is the same as that shown in Figs. 2 and 5. Dashed line shows zero-current level. (B) Current 7 ms after a step to  $+120$  mV is plotted vs. the holding voltage. Individual data from 14 different cells are shown. The pipette contained the standard pipette solution and the bath contained the standard CsCl extracellular solution. (C) Data for current at  $+120$  mV, shown in B, were normalized for each cell and the mean  $\pm$  SEM for 14 cells is shown. The data were normalized so that current after a holding voltage of  $+60$  mV is 0% and current after a holding voltage of  $-60$  mV is 100%.

mV (squares), and chord conductance for tail currents ( $G_{-80}$ ), measured immediately after voltage was returned to  $-80$  mV (diamonds), vs. pulse duration.  $G_{-80}$  is less than  $G_{120}$ , as expected from the outwardly rectifying instantaneous current-voltage relationship (Fig. 3). Both  $G_{120}$  and  $G_{-80}$  decrease as pulse duration increases. The decrease in  $G_{-80}$  indicates that depolarizing voltage steps did not activate an outward current nor a superimposed inward current. Diffusion polarization could cause the decay of currents at large positive voltages, but this would increase  $G_{-80}$



with increasing pulse duration;  $G_{-80}$  exhibits the opposite behavior. Fig. 5 *B* also shows the ratio of conductances ( $G_{120}:G_{-80}$ , triangles). Pulse duration has little effect on the conductance ratio. These observations indicate that Cl channels are open at  $-80$  mV and close with depolarization to  $+120$  mV.

Third, we examined the effect of holding voltage on whole-cell current. Fig. 6 *A* shows that as holding voltage was progressively depolarized, currents elicited by a voltage step to  $+120$  mV decreased. This observation can be quantified by plotting current immediately after the voltage step to  $+120$  mV vs. the holding voltage; Fig. 6 *B* shows results of similar experiments in 14 different cells. The data show that depolarization of the holding voltage decreased Cl current in all the cells, although the absolute amount of Cl current varied substantially from cell to cell. To facilitate graphical display, the data from Fig. 6 *B* was normalized and plotted in Fig. 6 *C*. The data indicate that depolarization of the holding voltage decreases Cl channel current.

In excised, inside-out patches from human tracheal epithelium we found that membrane voltage had variable effects on the probability of the apical membrane Cl channel being open (Welsh, 1986). However, some channels in excised patches clearly had kinetics similar to the whole-cell Cl currents, in that open channel probability was high at  $-80$  mV and progressively decreased during a 600-ms step to  $+120$  mV; an example is shown in Fig. 7. Fig. 7 *A* shows four consecutive sweeps that suggest that open channel probability decreases during the step to  $+120$  mV. The inset in the top left-hand corner demonstrates that what appears as an increase in the baseline noise at  $-80$  mV is actually the Cl channel, which is predominantly open with occasional closings. In each sweep the channel is open before the pulse to  $+120$  mV. In three of the four sweeps the channel closes during the voltage step and then reopens when the voltage is returned to  $-80$  mV. This is confirmed in Fig. 7 *B*, which shows the average of 127 sweeps made with the same protocol. The decrease in average current during the step is directly proportional to the decrease in open channel probability: the single-channel current amplitude ( $i$ ) would represent a probability of 1 and the zero-current level would represent a probability of 0.

#### *Isolation of Cl Currents*

To study the regulation and inhibition of the whole-cell Cl currents it would be ideal to isolate current flowing through apical membrane Cl channels, with no contribution from leak currents. Unfortunately, it was not technically possible to subtract leak currents because holding membrane voltage at large positive values for the required time (5 s or longer) frequently causes loss of the pipette-membrane seal. However, a rough estimate of leak current at negative voltage can be obtained from the tail current after the longest pulse shown in Fig. 5. An estimate of leak current at positive voltages can be obtained from the currents in Fig. 6 *A*, using current at a holding voltage of  $+60$  mV and current at  $+120$  mV after the holding voltage of  $+60$  mV (note that Fig. 5 and 6 *A* are from the same cell). Analysis such as this indicates that the leak current is roughly linear and reverses at  $\sim 0$  mV.

As the best practical method of isolating Cl current and controlling for time-dependent changes, we measured the current that decayed during a depolarizing voltage step. Our standard protocol for measuring decaying Cl current was to mea-

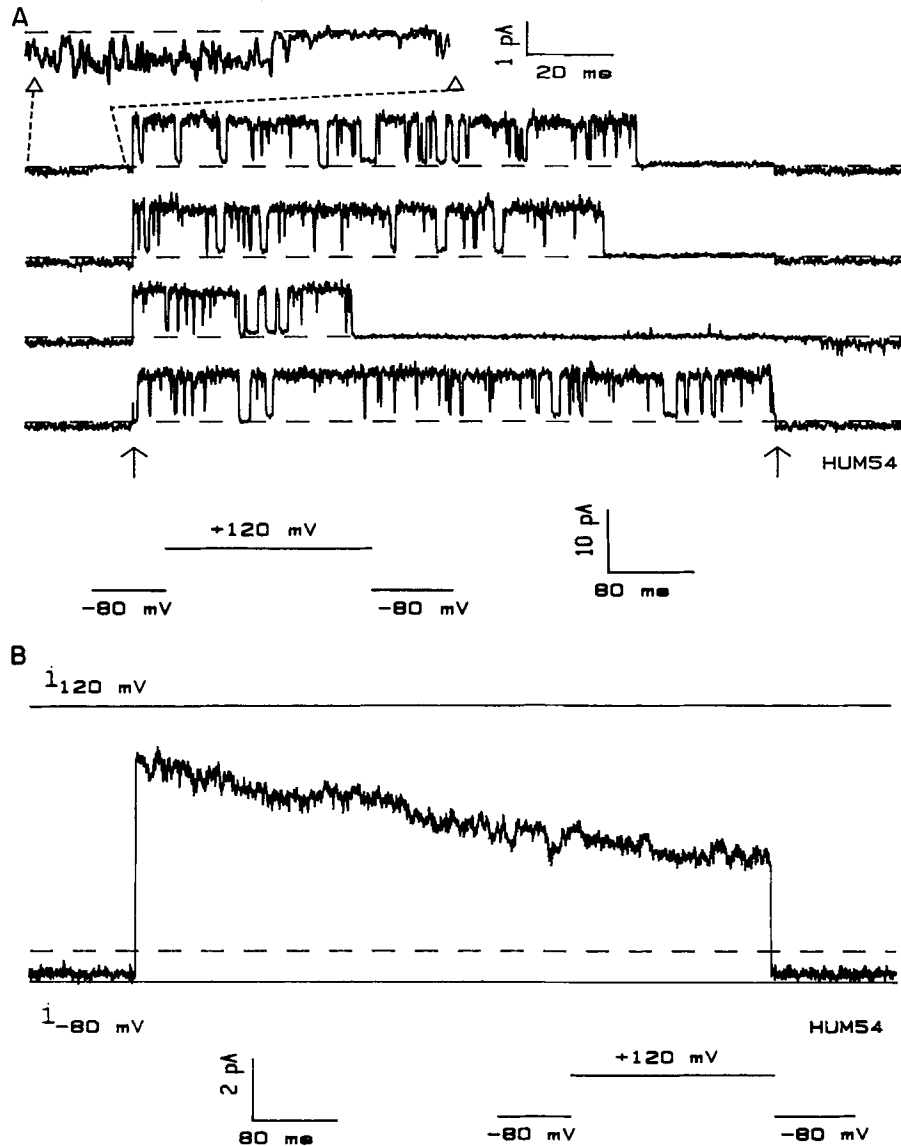


FIGURE 7. Effect of voltage on single-channel Cl currents. Tracings are from a single Cl channel studied in an excised, inside-out patch. Pipette solution was our standard extracellular solution and the bath contained 140 mM NaCl, 2 mM MgCl<sub>2</sub>, 5 mM EGTA (buffered to 100  $\mu$ M free Ca), 10 mM HEPES, pH 7.2. Capacitative and leak current was subtracted by using a sweep in which no channels were open. (A) Four consecutive sweeps are shown. Voltage was held at -80 mV and stepped to +120 mV for 600 ms. The inset in the upper-left corner is scaled current from the indicated portion of the first sweep. Arrows indicate the start and end of the voltage step. Dashed line indicates the zero-current level. (B) Average of 127 consecutive sweeps from the same patch and same protocol as in Fig. 6 A. Dashed line indicates the zero-current level and solid lines indicate single-channel current amplitude ( $i$ ) at +120 and -80 mV.

sure the difference in currents 7 and 595 ms after a step change in voltage from  $-80$  to  $+120$  mV.

An advantage of measuring decaying Cl current at  $+120$  mV is that cell-to-cell variability in currents resulting from differences in leak current are minimized. In addition, the current-voltage relationship for leak current is nearly linear but the current-voltage relationship for Cl channel current is outwardly rectifying. As a result, the ratio of Cl current to leak current is maximized during depolarizing pulses.

A disadvantage of measuring Cl current that decays during a 600-ms step to  $+120$  mV is that the decay is incomplete (see Fig. 6 A). Therefore this protocol underestimates total Cl current. Thus, values for decaying Cl current represent the relative amount of Cl current, not the absolute amount.

#### *Inhibition of Cl Currents by Cl Channel Blockers*

As another way of identifying the decaying Cl current as the one responsible for the apical Cl conductance, we examined the effect of agents that inhibit the Cl channel. In previous studies, we showed that two carboxylic acid analogues, anthracene-9-carboxylic acid and diphenylamine-2-carboxylate (DPC) inhibited apical Cl channels at concentrations similar to those required to inhibit Cl secretion in the native epithelium (Welsh, 1984, 1986a, b). To examine the effect of DPC on the whole-cell Cl current we measured the current that decayed during a 600-ms voltage step from  $-80$  to  $+120$  mV, 75 s after attaining the whole-cell recording mode. In these experiments the pipette contained either vehicle (DMSO) ( $n = 8$ ) or 2 mM DPC ( $n = 10$ ) in a solution of (in millimolar): 100 CsCl, 3 MgCl<sub>2</sub>, 1 MgATP, 10 EGTA, and 10 HEPES titrated to pH 7.2 with  $\sim 35$  CsOH. The bath contained our standard extracellular NaCl solution. Decaying Cl<sup>-</sup> current was inhibited 91% by 2 mM DPC ( $P < 0.005$  by an unpaired student's  $t$  test). For comparison, 2 mM DPC inhibited Cl secretion and single Cl channel current by 80–85% (Welsh, 1986b).

A more potent Cl<sup>-</sup> channel blocker, NPPB, has recently been reported to block single outwardly rectifying Cl channels in a Cl-secreting colonic tumor cell line (HT<sub>29</sub>) (Hayslett et al., 1987). To examine the effect of NPPB in airway cells, we mounted cultured monolayers of canine tracheal epithelial cells in Ussing chambers and added NPPB to the mucosal bathing solution. Cl secretory rate, as assessed by the short-circuit current, was  $21 \pm 4 \mu\text{A cm}^2$  before the addition of NPPB; 10  $\mu\text{M}$  inhibited  $60 \pm 13\%$  of the Cl current and 20  $\mu\text{M}$  inhibited  $85 \pm 5\%$  ( $n = 4$  monolayers). Fig. 8 shows that increasing concentrations of NPPB also inhibited the whole-cell Cl current. These results show that DPC and NPPB inhibit whole-cell Cl currents and Cl secretion at similar concentrations.

#### *Run-up and Run-down of Cl Channel Currents*

Typically after breaking into the whole-cell configuration, Cl currents increased with time ("run-up"), peaking several minutes after the beginning of the experiment, and then they would decrease ("run-down"). An example of this phenomenon is shown in Fig. 9 A. The observation that the absolute current (*crosses*) increases with time cannot be explained by an increase in leak current because the decaying current (*diamonds*) also increases with time. Although current measured at the end of a

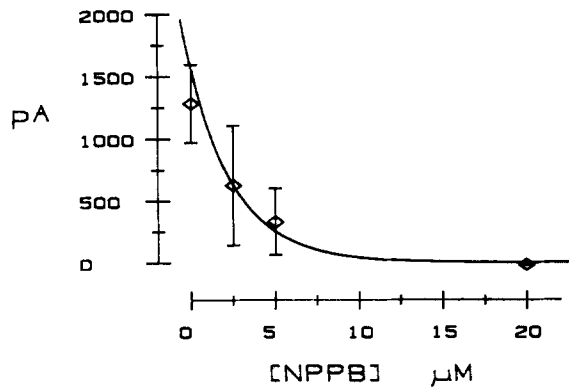


FIGURE 8. Effect of NPPB on Cl channel current. The pipette contained in millimolar: 100 CsCl, 3 MgCl<sub>2</sub>, 1 MgATP, 10 EGTA, and 10 HEPES titrated to pH 7.2 with approximately 35 CsOH. The bath contained our standard bath solution plus vehicle (DMSO) or the specified concentration of NPPB. The current that decayed when the voltage was stepped from -80 to +120 mV was normalized to mean current in the absence of NPPB. Data represents mean  $\pm$  SEM from at least five cells at each point. The line is derived from exponential regression on the data yielding a concentration at 50% inhibition of 3.1  $\mu$ M.

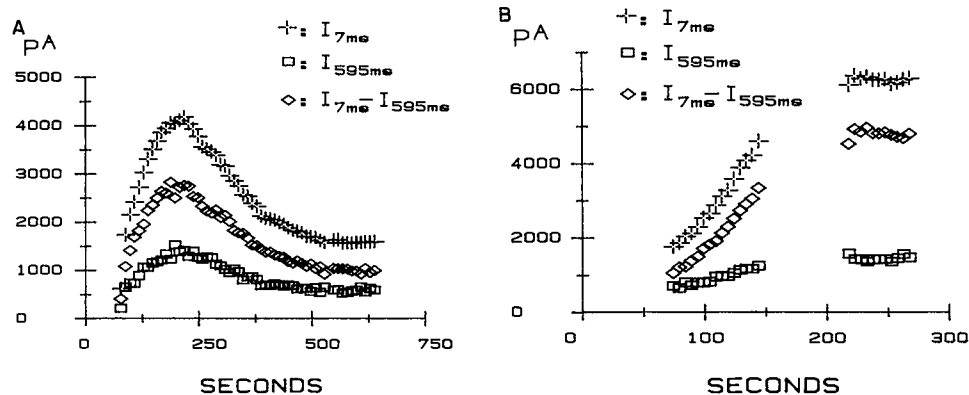


FIGURE 9. Spontaneous change in whole-cell current with time. (A) Holding voltage was -80 mV throughout and membrane voltage was stepped to +120 mV once every 10 s. Series resistance was rechecked frequently. Horizontal axis represents time after breaking into the cell. Values represent current measured 7 ms after the onset of the pulse to +120 mV (*crosses*), current measured 595 ms after the onset of a pulse to +120 mV (*squares*), and the difference between the current at 7 ms and current at 595 ms (*diamonds*). (B) The effect of depolarizing voltage steps on spontaneous increase in Cl current. The same protocol was used as in A except pulses were spaced at 5-s intervals and there is a 75-s pause during which no depolarizing pulses were given.

600-ms pulse (*squares*) also increased with time, this increase probably does not represent an increase in leak current because current at +120 mV did not completely decay during a 600-ms pulse (i.e., see Figs. 2, 5, and 6 A). After current increased, it then progressively decreased.

We tested the possibility that stepping voltage to +120 mV might open Cl channels and therefore be responsible for run-up of current. We were concerned about this possibility because in excised, single-channel experiments we found that depolarizing voltage steps (+120 mV) of several seconds in duration activated previously quiescent apical membrane Cl channels (Li et al., 1988). To address this concern, we altered the pulsing protocol. During an initial period, holding voltage was -80 mV and at 5-s intervals we gave 600-ms pulses to +120 mV to examine the initial rate of run-up. Then the depolarizing pulses were stopped for 45 s to 3 min while the holding voltage remained at -80 mV. We then resumed pulses to +120 mV. Fig. 9 B shows an example. In each experiment ( $n = 6$ ) run-up continued despite discontinuation of the depolarizing pulses. This observation suggests that run-up does not result from intermittent membrane depolarization.

Spontaneous run-up of Cl channel current poses a problem if one wishes to study Cl channel regulation. Therefore we did several experiments to determine its cause. To test the possibility that some constituent in the pipette solution may activate Cl channels we used a solution that contained more "physiologic" ion concentrations. The pipette solution contained, in millimolar: 80 K-aspartate, 45 KCl, 5 NaCl, 5 EGTA/20 KOH, 1 MgATP, and 10 MOPS/NaOH, pH 7.2. With this pipette solution and our standard NaCl bath solution, current still ran-up ( $n = 3$ ). To test whether protein phosphorylation or dephosphorylation might be responsible for Cl current run-up we removed ATP from the pipette solution ( $n = 2$ ), but still observed run-up. In separate experiments we also added 1 U/ml protein kinase inhibitor ( $n = 2$ ), 1 U/ml alkaline phosphatase ( $n = 2$ ), 10 mM phosphocreatine ( $n = 1$ ), 100  $\mu$ M GTP ( $n = 2$ ), and 5 mM dithiothreitol ( $n = 3$ ). None of these interventions prevented run-up.

We also considered the possibility that cell swelling might produce the changes in Cl current. We found that increasing extracellular osmolarity by 20 mosmol and decreasing pipette osmolarity by 10 mosmol prevented run-up of Cl currents. Thus, the rest of the experiments done to address regulation of Cl currents were done with bath solutions containing (in millimolar): 135 NaCl, 1.2 MgCl<sub>2</sub>, 1.2 CaCl<sub>2</sub>, 2.4 K<sub>2</sub>HPO<sub>4</sub>, 0.6 KH<sub>2</sub>PO<sub>4</sub>, 10 HEPES, and 10 dextrose and pipette solutions containing 135 CsCl, 2 MgCl<sub>2</sub>, 1 MgATP, 3 EGTA (nominal Ca<sup>2+</sup>), 10 HEPES (pH 7.2 with ~10 CsOH).

#### *Regulation of Cl Channel Current by Osmolarity*

Because altering the osmolarity of our solutions prevented Cl current run-up, we asked whether acutely decreasing extracellular osmolarity would activate Cl currents. Therefore we reduced extracellular osmolarity by decreasing bath NaCl concentration from 135 to 90 mM; as a result, the inactivating Cl current increased as shown in Fig. 10. This increase in current occurred despite a reduction in the chemical gradient for outward Cl current. (Note that in the absence of a change in Cl permeability, a reduction in external Cl concentration would decrease outward cur-

rent.) When extracellular NaCl concentration was increased back to 135 mM, there was initially a small increase in Cl current followed by a reduction to baseline values. The initial transient increase in outward current probably results from an increase in the chemical gradient for outward Cl current and the secondary reduction to baseline current is due to a decrease in Cl permeability. Six of seven cells studied with the same maneuver increased their inactivating Cl current at least 150% when NaCl was reduced from 135 to 90 mM.

This experimental intervention causes a change in both NaCl concentration and extracellular osmolarity. To determine which was responsible for stimulating Cl current we reduced the NaCl concentration from 135 to 90 mM while maintaining the extracellular osmolarity with sucrose or mannitol; in five of five cells we failed to

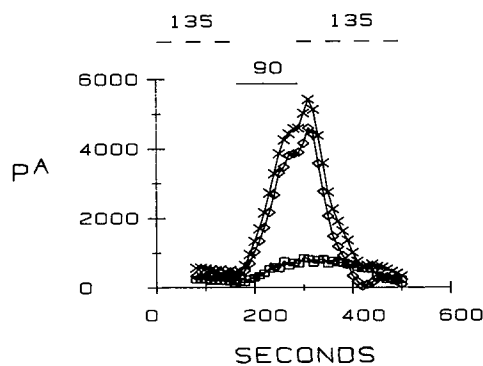


FIGURE 10. Effect of reducing extracellular osmolarity on Cl channel currents. The voltage protocol and symbol meanings are identical to those in Fig. 9. The pipette contained a solution identical to our standard extracellular solution except the EGTA concentration was reduced from 5 to 3 mM. The bath contained a solution identical to our standard bathing solution except for the addition of 2.4 mM  $K_2HPO_4$ , 0.6 mM  $KH_2PO_4$ , and 10 mM dextrose. Where indicated, bath NaCl concentration was reduced from 135 mM (*dashed line*) to 90 mM (*solid line*) and then returned to 135 mM (*dashed line*).

activate the Cl current. This observation suggests that it is the change in osmolarity that activates the Cl current.

In four experiments we reduced the CsCl concentration of the pipette solution from 135 to 90 mM. Under this condition, a reduction of the bath NaCl concentration from 135 to 90 mM failed to activate Cl currents. However, a further reduction in bath NaCl to 45 mM increased Cl current at least 150% in four of four experiments. These data indicate that it is not the absolute value of bath osmolarity that activates Cl currents but the osmotic gradient across the plasma membrane.

Changes in cell volume have not previously been reported to regulate the apical membrane Cl conductance of airway epithelium. Therefore we were concerned that these osmolarity-activated Cl currents might not flow through the apical membrane Cl channel. To address this concern we studied Cl secretion across monolayers of cells grown on permeable supports. Cells grown under these conditions are polar-

ized, so that an increase in the rate of transepithelial Cl secretion can readily be attributed to activation of apical membrane Cl channels. Fig. 11 shows that short-circuit current was stimulated when we reduced bath osmolarity by decreasing the NaCl concentration from 135 to 90 mM in both the mucosal and submucosal solutions. Short-circuit current increased from  $6.2 \pm 0.8$  to  $14.4 \pm 1.4 \mu\text{A}/\text{cm}^2$  (mean  $\pm$  SEM,  $n = 28$ ,  $P < 0.001$ ). Current increased despite a decrease in Cl concentration; reducing the NaCl concentration would, by itself, be expected to reduce short-circuit current. Moreover, because Cl concentration was decreased symmetrically, the results cannot be explained by the development of a diffusion voltage. Consequently the increase in current suggests stimulation of Cl secretion (note that amiloride was present in the mucosal bathing solution to inhibit Na absorption). The increase in current was transient, most likely as a result of cell volume regulatory

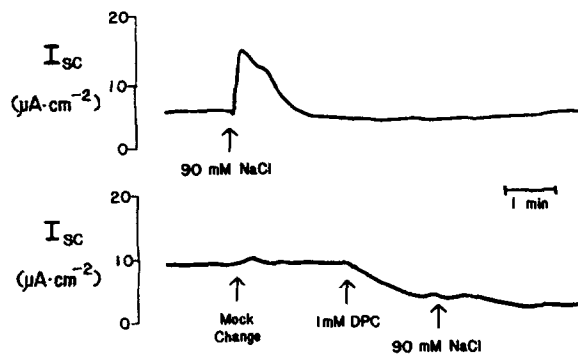


FIGURE 11. Effect of reduction of bath osmolarity on short-circuit current. (*Upper trace*) At the indicated time the NaCl concentration of both mucosal and submucosal baths was reduced from 135 to 90 mM by adding 1 ml of NaCl-free Ringers to 2 ml of a NaCl Ringers solution. (*Lower trace*) At the indicated time a mock solution change was made by adding 1 ml of NaCl Ringers to 2 ml of NaCl Ringers. Where indicated, 1 mM DPC was added to the mucosal bathing solution and then mucosal and submucosal NaCl concentrations were reduced from 135 to 90 mM.

mechanisms that restore cell volume even in the presence of an altered extracellular osmolarity.

Fig. 12 shows that the increase in short-circuit current was inhibited 95% in Cl-free solutions, 98% by mucosal addition of the Cl channel antagonist DPC, and 72% by submucosal addition of the NaCl cotransport inhibitor bumetanide. These data indicate that a reduction in bath osmolarity stimulates short-circuit current by stimulating transepithelial Cl secretion. Stimulation of Cl secretion requires an increase in apical membrane Cl conductance, i.e., an activation of apical Cl channels, and could not result from activation of basolateral Cl channels. Therefore we conclude that a reduction in bath osmolarity activates apical membrane Cl channels in the intact epithelium just as a reduction in bath osmolarity activates whole-cell Cl currents.

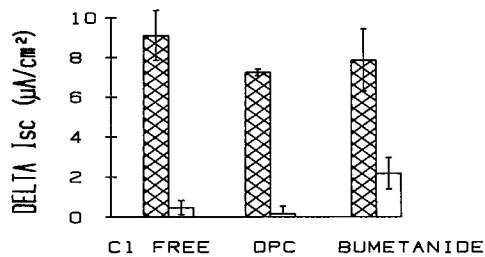


FIGURE 12. Effect of Cl transport inhibitors on change in short-circuit current ( $I_{sc}$ ) induced by osmolarity reduction. For each set of studies, we reduced the bath NaCl concentration from 135 to 90 mM on a pair of monolayers, one served as a control (cross-hatched bars) and one received the experimental intervention (open bars). Values represent the change in  $I_{sc}$  resulting from the reduction in NaCl. For Cl-free solutions Cl was replaced by gluconate ( $n = 8$  pairs); DPC (1 mM) was added to the mucosal solution ( $n = 5$  pairs); bumetanide (100  $\mu$ M) was added to the submucosal solution ( $n = 8$  pairs). The experimental intervention significantly reduced the response in each case ( $P < 0.03$ ).

#### Regulation of Cl Currents by cAMP-dependent Protein Kinase

Considerable evidence suggests an important role for cAMP in regulating apical membrane Cl permeability (Welsh, 1987b). Because many of the cellular effects of cAMP are mediated by activation of cAMP-dependent protein kinase (Nestler and Greengard, 1984; Levitan, 1985), we asked whether purified catalytic subunit of cAMP-dependent protein kinase (0.01 U/ml) would increase whole-cell Cl currents.

Fig. 13 shows the effect of the catalytic subunit of cAMP-dependent protein kinase on the decaying Cl channel current. The measurement was made 2.5 min after breaking into the cell. Currents were compared between cells in which the pipette solution did or did not contain the catalytic subunit of cAMP-dependent

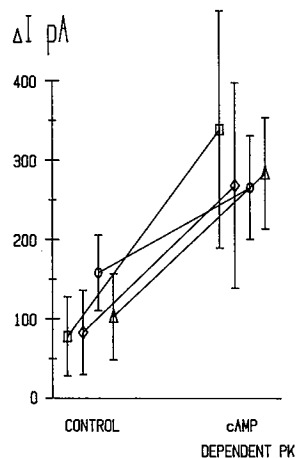


FIGURE 13. Effect of the catalytic subunit of cAMP-dependent protein kinase on Cl channel current. Decaying Cl current was measured 2.5 min after breaking into the whole-cell mode. Data points represent means  $\pm$  SEM of decaying Cl current ( $\Delta I$ ) from at least five cells. Cells from four subjects were studied with or without catalytic subunit (75 nM) in the pipette. Cell capacitance was  $28.3 \pm 2.3$  pF ( $n = 22$ ) for controls and  $29.2 \pm 1.5$  pF ( $n = 20$ ) for cells perfused with the catalytic subunit. Series resistance was  $7.15 \pm 0.15$  M $\Omega$  ( $n = 22$ ) for controls and  $6.44 \pm 0.56$  M $\Omega$  ( $n = 20$ ) for experimentals.



protein kinase (0.01 U/ml). For each group of cells the average Cl current is greater in cells perfused with catalytic subunit plus ATP than in cells perfused with ATP alone. Inactivating Cl current was  $103 \pm 25$  pA ( $n = 22$ ) in control cells and  $290 \pm 51$  pA ( $n = 20$ ) ( $P = 0.002$  by unpaired  $t$  test) when the pipette contained catalytic subunit. Peak whole-cell current measured 7 ms after stepping to +120 mV was  $315 \pm 68$  pA ( $n = 22$ ) in control cells and increased to  $602 \pm 99$  pA ( $n = 20$ ) ( $P = 0.02$  by unpaired  $t$  test) when catalytic subunit was included in the pipette solution. These data indicate that cAMP-dependent protein kinase increases Cl channel current.

## DISCUSSION

### *Whole-Cell Cl Channel Currents*

Several observations suggest that the whole-cell Cl currents flow through the apical membrane Cl channel in human airway epithelium. First, the conductive properties of the whole-cell currents are similar to the conductive properties of the apical membrane Cl channel studied with the single-channel patch-clamp technique (Welsh, 1986*a, b*; Frizzell et al., 1986): both show current rectification in the outward direction in the presence of symmetrical Cl concentrations. For example, compare the current-voltage relationship in our Fig. 3 with the single-channel current-voltage relationship of Fig. 1 in Welsh, 1986*a* or of Fig. 2*B* in Welsh and Liedtke, 1986. Second, Cl channel blockers inhibited whole-cell current at concentrations similar to those required to inhibit Cl secretion. Third, regulation of whole-cell currents, regulation of single, apical membrane Cl channels, and regulation of the apical membrane Cl permeability in native and cultured epithelia is similar: reduction in extracellular osmolarity and cAMP, or cAMP-dependent protein kinase, activate apical membrane Cl channels (Welsh, 1986*a, b*, 1987*b*; Schoumacher et al., 1987; Li et al., 1988).

In our studies, the instantaneous (Fig. 3) and steady-state (Fig. 6, *B* and *C*) current-voltage relationships indicate that the outwardly rectifying Cl channel, which closes with large depolarization, is the predominant Cl-conductive pathway in the cell membrane. Although other Cl channels may be represented in the whole-cell current, they would appear to make only a small contribution to membrane conductance. For example, after membrane voltage was held at +60 mV to allow Cl current to decay, cells often had an input resistance of 1 G $\Omega$ , indicating that the membrane is electrically tight when Cl channels are closed (e.g., see Fig. 6, *A* and *B*).

In previous studies using the single-channel patch-clamp technique, we have focused on a single type of Cl channel (Welsh, 1986*a, b*; Welsh and Liedtke, 1986; Li et al., 1988) that showed outward current rectification and had a single-channel conductance of ~25–30 pS measured as the slope conductance at 0 mV. (Note that because the single-channel current-voltage relationship is not linear, there is no unique value of single-channel conductance.) That particular channel is activated by hormonal stimuli and is abnormally regulated in cystic fibrosis airway epithelial cells. A lower conductance (~20 pS) anion-selective channel with a linear current-voltage relationship has also been reported in human airway cells (Frizzell et al., 1986). However it was observed much less frequently than the outwardly rectifying Cl channel. Previous studies in native and cultured airway epithelia indicate that the

cellular Cl conductance is located in the apical membrane (Welsh et al., 1982; Shorofsky et al., 1983, 1984; Welsh, 1985b).

#### *Activation of the Cl Channel*

It is interesting to consider the mechanisms of activation of the Cl channel in light of the present findings and in light of previous studies on single channels and cell monolayers. An understanding of such mechanisms is particularly important because in the disease cystic fibrosis, activation of Cl channels is defective (Widdicombe et al., 1985; Frizzell et al., 1986; Welsh and Liedtke, 1986; Schoumacher et al., 1987; Li et al., 1988).

First, the channel is activated by cAMP. Our results show that catalytic subunit of cAMP-dependent protein kinase, in the presence of ATP, increases whole-cell Cl current. Activation of the Cl channel by the cAMP-dependent protein kinase was expected from previous work in the native and cultured epithelia. Application of the catalytic subunit of the cAMP-dependent protein kinase to whole-cell and to excised patches (Schoumacher et al., 1987; Li et al., 1988) mimics the increase in apical membrane Cl permeability that follows the addition of secretagogues or cAMP to native and cultured epithelia (Welsh et al., 1982; Shorofsky et al., 1983; Welsh, 1985b). These results indicate that the Cl channel protein, or a regulatory protein closely associated with the channel, is phosphorylated, resulting in activation of the channel.

Second, Ca may play some role in regulating the channel, however, its role is not understood. In cultured monolayers (Widdicombe, 1986) and with cell-attached patches (Frizzell et al., 1986; unpublished observations) the channel can be activated by the calcium ionophore A23187. However, in canine tracheal epithelium, indomethacin prevents the stimulatory effect of A23187 in native cells and attenuates the effect in cultured cells, indicating that intracellular Ca may indirectly regulate the apical membrane Cl<sup>-</sup> conductance via prostaglandin synthesis (Welsh, 1987a). In previous studies, we found that changes in internal Ca did not activate Cl channels in excised, inside-out patches (Welsh, 1986a, b). In another report using excised, inside-out patches, internal Ca did show some variable regulation of the channel (Frizzell et al., 1986). Previous reports show that the channel can be activated by cAMP-dependent protein kinase or membrane depolarization at Ca concentrations below resting cellular levels (Schoumacher et al., 1987; Li et al., 1988). In the present experiments, cAMP-dependent protein kinase and reduced osmolarity activated Cl channels at internal Ca concentrations of 10 nM, as well as when the pipette contained 10 mM EGTA with no added Ca. Thus it seems that elevation of cytosolic Ca above basal levels is not necessary for channel activation, but Ca may be involved at some point in regulation.

Third, our results show that reducing bath osmolarity activates the channel. Such activation occurs in the absence of cAMP-dependent protein kinase or ATP and is independent of membrane depolarization. One question that this form of channel activation raises is: do changes in the level of some second messenger (e.g., cAMP or Ca<sup>2+</sup>) couple changes in osmolarity to activation of Cl currents?

It seems unlikely that osmotic effects on the channel result from an effect on cAMP, because run-up of Cl channels occurred when cells were perfused with the cAMP-dependent protein kinase inhibitor. Moreover, similar changes in osmolarity

do not result in measurable increases in cellular levels of cAMP (unpublished observations).

It also seems unlikely that increases in intracellular  $\text{Ca}^{2+}$  concentration couple a decrease in osmolarity to activation of Cl channels, because reducing osmolarity activated Cl channels when the pipette contained a  $\text{Ca}^{2+}$  concentration buffered at one tenth the normal cytosolic  $\text{Ca}^{2+}$  concentration (basal levels  $\sim 100$  nM, McCann et al., 1988). Moreover, a reduction in osmolarity stimulated the inactivating Cl current even in the absence of extracellular  $\text{Ca}^{2+}$  (unpublished observations).

How then is a decrease in extracellular osmolarity coupled to Cl channel activation? We speculate that the osmotic changes cause cell swelling. This is consistent with our observation that it is the osmotic gradient across the cell and not the absolute level of bath osmolarity that stimulates Cl currents. These findings are also consistent with our previous report that increasing basolateral K concentrations increases apical Cl conductance and stimulates Cl secretion (Welsh, 1985a). We speculate that an increase in the basolateral K concentration may have also caused cell swelling. If it is cell swelling that activates the channel, an interaction of the cell cytoskeleton with the channel may be responsible. We do not know whether osmotic changes play any physiologic role in regulation of Cl secretion. This point will require measurements of cell volume under a variety of conditions.

Certainly further work is needed to elucidate the mechanisms by which the channel is activated. Use of the whole-cell patch-clamp technique may be especially valuable for understanding such mechanisms and in further addressing defective regulation in cystic fibrosis.

#### *Voltage Dependence of the Cl Channel*

Our data show that Cl current decays, i.e., channels close, with membrane depolarization. It is difficult to directly compare the voltage dependence of whole-cell Cl currents and the voltage dependence of Cl channels in excised patches. (Note that here we are discussing the effect of voltage on channels already activated; voltage-induced activation of excised Cl channels was discussed above.) Although the rate of decay varied from one preparation to another, whole-cell currents consistently decayed with depolarization to +90 or +120 mV. In contrast, we found that the probability of a channel being open in an excised, inside-out patch was variable (Welsh, 1986a, b). However,  $\sim 10\%$  of excised Cl channels clearly showed a voltage dependence similar to that found in whole-cell recordings (i.e., Fig. 7). In contrast, when studying canine tracheal epithelial cells we find that Cl channels studied with the single-channel and whole-cell techniques show similar responses to voltage.<sup>1</sup>

<sup>1</sup> In this study we show Cl currents from normal human cells, however, we have obtained identical whole-cell results with canine tracheal epithelial cells. In addition, with excised inside-out patches of canine tracheal cells, we consistently find (90% of studies) that membrane depolarization decreases open channel probability (when studied with experimental conditions identical to those used for Fig. 7). This voltage-dependent decrease in open-state probability is observed with channels activated by either strong membrane depolarization or by the catalytic subunit of the cAMP-dependent protein kinase. It is not clear why voltage effects on channel kinetics are more variable in excised patches from human cells than in patches from canine cells. However, the concordance of the data from canine whole-cell and excised patch recordings provides further evidence that the two techniques study the same channel.

Despite some variability in the voltage dependence of Cl channels studied with the whole-cell and single-channel techniques, the similarities in conductive properties and regulation suggest that both methods record current from the same population of channels. It is possible that either method might cause functional changes in Cl channels that are reflected as a difference in voltage dependence. There are several examples in which channel kinetics appear different when channels are studied under different conditions. For example, outside-out patches from rat myotubes contain acetylcholine channels with similar conductive properties but different kinetic properties than acetylcholine channels in inside-out or cell-attached patches (Trautmann and Siegelbaum, 1983). Another example is found with Ca channels: under many experimental conditions they rapidly become completely inactive (Brown et al., 1982; Fenwick et al., 1982). The properties of stretch-activated channels are also altered by the pipette-membrane interaction and excision of the patch from the cell (Methfessel et al., 1986). Because the properties of stretch-activated channels appear to be dependent on interactions between the cytoskeleton and the channel, those results suggest a possible explanation for the variable effects of voltage on excised airway Cl channels. Our results, showing an effect of osmolarity on Cl channels, raise the possibility of channel-cytoskeleton interactions. Perhaps the excision of membrane patches alters the channel's interaction with the cytoskeleton thereby altering channel kinetics.

It is unknown whether the voltage dependence of the channel has any physiological role in regulating apical membrane Cl permeability. The electrical potential difference across the apical membrane of native and cultured tracheal epithelium under open-circuit conditions is  $-40$  to  $-50$  mV. With maximal stimulation of secretion, Cl channels open, thereby depolarizing the apical membrane by  $\sim 10$  mV. Data in Fig. 6 C suggest that this would have only minor effects on open channel probability. However, the voltage dependence of whole-cell Cl currents measured at nonphysiologic voltages should prove valuable as a marker for Cl channel current in future studies.

We thank Drs. Angus C. Nairn and Paul Greengard (Laboratory of Molecular and Cellular Neuroscience, Rockefeller University) for generously providing us with the purified catalytic subunit of cAMP-dependent protein kinase. We thank Phil Karp for technical assistance.

This work was supported by grants from the National Heart, Lung and Blood Institute (HL-29851 and HL-42385) and the Cystic Fibrosis Foundation. J. D. McCann is a March of Dimes Graduate Research Fellow.

*Original version received 28 March 1988 and accepted version received 8 May 1989.*

#### REFERENCES

- Brown, A. M., H. Camerer, D. L. Kunze, and H. D. Lux. 1982. Similarity of unitary Ca currents in three different species. *Nature*. 299:156–158.
- Coleman, D. L., I. K. Tuet, and J. H. Widdicombe. 1984. Electrical properties of dog tracheal epithelial cells grown in monolayer culture. *American Journal of Physiology*. 246:C355–C359.
- Fenwick, E. M., A. Marty, and E. Neher. 1982. Sodium and calcium channels in bovine chromaffin cells. *Journal of Physiology*. 331:599–635.

- Frizzell, R. A., G. Rechkemmer, and R. L. Shoemaker. 1986. Altered regulation of airway epithelial cell chloride channels in cystic fibrosis. *Science*. 233:558–560.
- Hamill, O. P., A. Marty, E. Neher, B. Sakmann, and F. J. Sigworth. 1981. Improved patch-clamp techniques for high-resolution current recording from cells and cell-free membrane patches. *Pflügers Archiv*. 391:85–100.
- Hayslett, J. P., H. Gogelein, K. Kunzelmann, and R. Greger. 1987. Characteristics of apical chloride channels in human colon cells (HT<sub>29</sub>). *Pflügers Archiv*. 410:487–494.
- Kaczmarek, L. K., K. R. Jennings, F. Strumwasser, A. C. Nairn, U. Walter, F. Wilson, and P. Greengard. 1980. *Proceedings of the National Academy of Sciences*. 77:7487–7491.
- Levitan, I. B. 1985. Phosphorylation of ion channels. *Journal of Membrane Biology*. 87:177–190.
- Li, M., J. D. McCann, C. M. Liedtke, A. C. Nairn, P. Greengard, and M. J. Welsh. 1988. cAMP-dependent protein kinase opens chloride channels in normal but not cystic fibrosis airway epithelium. *Nature*. 331:358–360.
- Marty, A., and E. Neher. 1983. Tight-seal whole-cell recording. In *Single-Channel Recording*. B. Sakmann and E. Neher, editors. Plenum Publishing Corp., New York.
- McCann, J. D., R. C. Bhalla, and M. J. Welsh. 1989. Release of intracellular calcium by two different second messengers in airway epithelium. *American Journal of Physiology: Lung Cellular and Molecular Physiology*. 257:L116–L124.
- Methfessel, C., V. Witzemann, T. Takahashi, M. Mishina, S. Numa, and B. Sakmann. 1986. Patch clamp measurements on *Xenopus laevis* oocytes: currents through endogenous channels and implanted acetylcholine receptor and sodium channels. *Pflügers Archiv*. 407:577–588.
- Nestler, E. J., and P. Greengard. 1984. *Protein Phosphorylation in the Nervous System*. John Wiley and Sons, New York.
- Schoumacher, R. A., R. L. Shoemaker, D. R. Halm, E. A. Tallant, R. W. Wallace, and R. A. Frizzell. 1987. Phosphorylation fails to activate chloride channels from cystic fibrosis airway cells. *Nature*. 330:752–754.
- Shorofsky, S. R., M. Field, and H. A. Fozzard. 1983. Electrophysiology of Cl secretion in canine trachea. *Journal of Membrane Biology*. 72:105–115.
- Shorofsky, S. R., M. Field, and H. A. Fozzard. 1984. Mechanism of Cl secretion in canine trachea: changes in intracellular chloride activity with secretion. *Journal of Membrane Biology*. 81:1–8.
- Trautmann, A., and S. A. Siegelbaum. 1983. The influence of membrane patch isolation on single acetylcholine-channel current in rat myotubes. In *Single-Channel Recording*. B. Sakmann and E. Neher, editors. Plenum Publishing Corp., New York. 473–480.
- Welsh, M. J. 1984. Anthracene-9-carboxylic acid inhibits an apical membrane chloride conductance in canine tracheal epithelium. *Journal of Membrane Biology*. 78:61–71.
- Welsh, M. J. 1985a. Basolateral membrane potassium conductance is independent of sodium pump activity and membrane voltage in canine tracheal epithelium. *Journal of Membrane Biology*. 84:25–33.
- Welsh, M. J. 1985b. Ion transport by primary cultures of canine tracheal epithelium: methodology, morphology, and electrophysiology. *Journal of Membrane Biology*. 88:149–163.
- Welsh, M. J. 1986a. An apical-membrane chloride channel in human tracheal epithelium. *Science*. 232:1648–1650.
- Welsh, M. J. 1986b. Single apical membrane anion channels in primary cultures of canine tracheal epithelium. *Pflügers Archiv*. 407:116–122.
- Welsh, M. J. 1987a. Effect of phorbol ester and calcium ionophore on chloride secretion in canine tracheal epithelium. *American Journal of Physiology*. 253:C828–C834.
- Welsh, M. J. 1987b. Electrolyte transport by airway epithelia. *Physiological Reviews*. 67:1143–1184.

- Welsh, M. J., and C. M. Liedtke. 1986. Chloride and potassium channels in cystic fibrosis airway epithelia. *Nature*. 322:467-470.
- Welsh, M. J., P. L. Smith, and R. A. Frizzell. 1982. Chloride secretion by canine tracheal epithelium: II. The cellular electrical potential profile. *Journal of Membrane Biology*. 70:227-238.
- Widdicombe, J. H. 1986. Cystic fibrosis and beta-adrenergic response of airway epithelial cell cultures. *American Journal of Physiology*. 251:R818-R822.
- Widdicombe, J. H., M. J. Welsh, and W. E. Finkbeiner. 1985. Cystic fibrosis decreases the apical membrane chloride permeability of monolayers cultured from cells of tracheal epithelium. *Proceedings of the National Academy of Sciences*. 82:6167-6171.